Development 126, 23-36 (1999)
Printed in Great Britain © The Company of Biologists Limited 1998
DEV3899

NeuroD regulates multiple functions in the developing neural retina in rodent

Eric M. Morrow[1], Takahisa Furukawa[1], Jacqueline E. Lee[2] and Constance L. Cepko[1,*]

[1]Department of Genetics and Howard Hughes Medical Institute, Harvard Medical School, 200 Longwood Avenue, Boston, Massachusetts 02115, USA
[2]Department of Molecular, Cellular and Developmental Biology, Campus Box 347, University of Colorado, Boulder, Colorado 80309, USA
*Author for correspondence (e-mail: cepko@rascal.med.harvard.edu)

Accepted 14 October; published on WWW 3 December 1998

SUMMARY

The expression and function of the basic helix-loop-helix (bHLH) transcription factor NeuroD were studied in the developing neural retina in rodent. *neuroD* was expressed in areas of undetermined retinal cells as well as developing photoreceptors and amacrine interneurons. Expression was maintained in a subset of mature photoreceptors in the adult retina. Using both loss-of-function and gain-of-function approaches, NeuroD was found to play multiple roles in retinal development. (1) NeuroD was found to be a critical regulator of the neuron versus glial cell fate decision. Retinal explants derived from NeuroD-null mice demonstrated a three- to fourfold increase in Müller glia. Forced expression of *neuroD* in progenitors in rat using retroviruses hastened cell cycle withdrawal and blocked gliogenesis in vivo. (2) NeuroD appeared to regulate interneuron development, favouring amacrine over bipolar differentiation. Forced NeuroD expression resulted in an increase in amacrine interneurons and a decrease in bipolar interneurons. In the complementary experiment, retinae derived from NeuroD-null mice demonstrated a twofold increase in bipolar interneurons and a delay in amacrine differentiation. (3) NeuroD appeared to be essential for the survival of a subset of rod photoreceptors. In conclusion, these results implicate NeuroD in a variety of developmental functions including cell fate determination, differentiation and neuron survival.

Key words: NeuroD, Retina, Glia, Interneuron development, Photoreceptor

INTRODUCTION

The vertebrate central nervous system (CNS) contains an amazing diversity of functionally and morphologically distinct cell types, broadly classified into neurons and glia. This cellular diversity is generated from the progenitor cells comprising the neural tube, by complex developmental mechanisms including cell proliferation, cell type specification and differentiation, and cell survival. The molecular mechanisms controlling these processes are areas of active study.

The neural retina offers several advantages as a model system in which to investigate the mechanisms of cell fate determination in the vertebrate CNS (reviewed by Cepko et al., 1996; Harris, 1997). The six classes of neurons and one glial cell class are generated in precise ratios and are well-characterized morphologically and biochemically. These cells form a trilaminated sheet of neural tissue consisting of: the photoreceptors (rods and cones) in the outer nuclear layer (ONL); the interneurons (amacrine, bipolar and horizontal cells) and the Müller glia, the cell bodies of which are found in the inner nuclear layer (INL); and the projection neurons (ganglion cells), which comprise the innermost cell layer, the ganglion cell layer (GCL).

Two lines of experiments have provided considerable insight into cell type specification in the vertebrate retina. First, birthdating studies have demonstrated that the seven retinal cell types are generated in an evolutionarily conserved order during development, although multiple cell types are simultaneously produced at any given developmental stage (reviewed by Altshuler et al., 1991). Second, lineage analysis has shown that retinal cells, including both neurons and glia, arise from common progenitors (Turner and Cepko, 1987; Holt et al., 1988; Wetts and Fraser, 1988; Turner et al., 1990; Fekete et al., 1994). In addition, lineage analysis also supports the idea that commitment to a given cell fate may occur during or after the terminal mitosis, since two-cell clones were found where each of the cells was of a different type. For example, clones containing one rod photoreceptor and one Müller glial cell were observed (Turner and Cepko, 1987). While the patterns of cell specification were thus elucidated, the molecular mechanisms that determine the cell fates of these postmitotic cells remain poorly understood.

The basic helix-loop-helix (bHLH) transcription factors play important roles in cell fate determination and differentiation across diverse systems, including *Drosophila* neurogenesis (reviewed by Jan and Jan, 1993; Campos-Ortega, 1993), vertebrate myogenesis (reviewed by Weintraub, 1993) and hematopoiesis (Porcher et al., 1996). In recent years, a large number of positively and negatively regulating bHLH genes have been identified in vertebrates and

shown to be expressed in the developing CNS (reviewed by Lee, 1997; Kageyama and Nakanishi, 1997). By gene targeting in mouse, some of the positively regulating bHLH proteins have been shown to be necessary for certain neuronal lineages and non-essential for others, probably due to redundancy (Guillemot et al., 1993; Ben-Arie et al., 1997; Naya et al., 1997; Fode et al., 1998; Ma et al., 1998; Schwab et al., 1998). Further, these bHLH factors have also been studied by overexpression in *Xenopus* embryos where ectopic expression promotes neurogenesis (Zimmerman et al., 1993; Turner and Weintraub, 1994; Ferreiro et al., 1994; Lee et al., 1995; Ma et al., 1996; McCormick et al., 1996; Takebayashi et al., 1997). To date, both gain-of-function and loss-of-function studies have rarely been undertaken in the same tissue. Such an analysis was performed in the retina for the negatively regulating bHLH HES-1 (Tomita et al., 1996a). Forced expression of HES-1 in retinal progenitors resulted in a blockage of neuronal differentiation. Further, targeted disruption of *HES-1* resulted in an upregulation of positively regulating bHLH genes and premature neuronal differentiation, including precocious expression of rhodopsin.

At least three positive-acting bHLH genes are expressed during postnatal rodent retinal development: *Mash1* (Johnson et al., 1990; Guillemot et al., 1993; Jasoni and Reh, 1996), *ATH-3* (Takebayashi et al., 1997), and *neuroD/BETA2* (Lee et al., 1995; Naya et al. 1995). In this report, we studied the expression and function of NeuroD in the developing rodent retina. *neuroD* is a member of a subfamily of bHLH genes, whose expression is detected late in neurogenesis, usually during and/or after the terminal mitosis of neural precursors (reviewed in Lee, 1997). Due to this expression pattern, NeuroD has been hypothesized to function largely in neuronal differentiation rather than determination (Lee et al., 1997; Fode et al., 1998; Ma et al., 1998). This proposal, however, remains to be studied thoroughly, particularly in regions of the developing nervous system where specification continues after the terminal mitosis, such as in the retina (Adler and Hatlee, 1989; Altshuler and Cepko, 1992; Belecky-Adams et al., 1996; Ezzeddine et al., 1997). *neuroD/BETA2* is also expressed in developing endocrine cells of the pancreas and gut (Naya et al., 1995). NeuroD-null mice exhibit defects in the development of these cells, and die within 5 days after birth with severe hyperglycemia (Naya et al., 1997; Mutoh et al., 1998; J. E. Lee et al., unpublished). No abnormalities to date have been indentified in the nervous system of the NeuroD-null mice upon gross examination, but late aspects of neural development have not been previously examined.

The goal of the current study was, therefore, to address the following two questions concerning the function of NeuroD in late rodent retinogenesis. (1) Does NeuroD play a role in regulating the neuron versus glia decision in the developing retina? (2) Does NeuroD influence the determination, differentiation and/or survival of specific neuron classes? To address these questions, loss-of-function studies were conducted in culture on neonatal tissue derived from NeuroD-null mice, and gain-of-function studies were conducted using retroviruses in vivo. Our results indicate that in the developing postnatal retina, NeuroD is involved in various developmental mechanisms, including the neuron/glia decision, interneuron subtype specification and photoreceptor survival.

MATERIALS AND METHODS

Rats

Timed-pregnant Sprague-Dawley rats were purchased from Taconic (Germantown, NY).

neuroD/BETA2 mutant mice

The entire coding region of the *neuroD* gene was replaced by the *lacZ* gene using homologous recombination (J. E. Lee et al., unpublished). Loss of *neuroD* RNA was confirmed by in situ hybridization (data not shown). Chimeric mice were mated to the C57BL/6 inbred strain. Genotyping was performed by Southern blotting. Tail genomic DNA was digested with *Eco*RI. A 1.4 kb fragment from the promoter region of the *neuroD* gene was used as a probe. The mutant allele was confirmed by a 6 kb diagnostic band and the wild type by a 4 kb band (data not shown).

In situ hybridization and riboprobes

Non-radioactive section in situ hybridization was performed as described previously (Riddle et al., 1993). Probe for *neuroD* was 1.7 kb of 3′ region of murine *neuroD* cDNA (Lee et al., 1995).

β-galactosidase histochemistry

Staged retinae from pups heterozygous for the *neuroD* knock-out/*lacZ* knock-in allele were collected and stained for β-galactosidase activity in whole mounts as described previously (Cepko et al., 1998), prior to embedding in 30% sucrose, freezing in OCT Compound (Tissue Tek) and cryosectioning.

Mouse retinal explant culture

Retinae were harvested from pups born to parents heterozygous for the mutant *neuroD* allele shortly after birth, prior to the onset of hyperglycemia. Mouse blood glucose levels were tested using Glucostix (Bayer) reagent strips. At this stage, genotype could not be determined by observation of pup; therefore, tail genomic DNA was prepared. Genotype was determined by Southern blotting as described above.

Explant culture was performed as described previously (Ezzeddine et al., 1997). Briefly, retinae were dissected free of surrounding ocular tissue. To minimize contamination by endothelial cells and astrocytes, blood vessels and retinal tissue surrounding the optic nerve were removed. Retinae were transferred to nucleopore polycarbonate membranes, 0.2 μm pore size (Costar Nucleopore, Charlotte, NC), and cultured in 45% DMEM, 45% Ham's FI2 Nutrient Mixture (Life Technologies), 10% FCS and penicillin streptomycin (100 U/ml) at 37°C and 5% CO_2 for 3-17 days. At the end of the culture period, explants were dislodged from the membranes, fixed immediately or dissociated as described previously (Morrow et al., 1998), and processed for immunohistoochemistry. BrdU-labelling of retinal explants for detection of cells in S phase was performed as described previously (Morrow et al., 1998).

Immunohistochemistry and antibodies

Dissociated cells were plated on poly-D-lysine (Sigma)-coated, eight-well glass slides (Cel-Line Associates, Newfield, NJ). Slides with cells were maintained at 37°C and 5% CO_2 for 1.5 hours prior to fixation. Retinal cells were fixed and processed for immunocytochemistry with differences in procedure depending on the antibody. For the following antibodies, tissue was fixed with 4% paraformaldehyde for 10 minutes and blocked in 2% donkey serum (Jackson ImmunoResearch, West Grove, PA), 2% goat serum (Jackson ImmunoResearch), and 0.1% Triton X-100 (Sigma): anti-rhodopsin, Rho4D2 (mouse monoclonal, 1:250; Molday, 1989); anti-cellular retinaldehyde binding protein (CRALBP) (rabbit polyclonal, 1:5000 dilution; De Leeuw et al., 1990); anti-γ-aminobutyric acid transporter-1 (GAT-1) (rabbit polyclonal, 1:300; Chemicon); anti-recoverin (rabbit polyclonal, 1:1000; Dizhoor et al., 1991); VC1.1 (mouse monoclonal, 1:1000; Sigma); and anti-β-galactosidase (rabbit polyclonal, 1:50; 5-prime-3-prime, Boulder, CO). For the following antibodies, tissue was fixed with 1%

paraformaldehyde for 10 minutes and blocked in 2% donkey serum and 0.02% Triton X-100: anti-glial fibrillary acidic protein (GFAP) (mouse monoclonal, 1:400; Sigma), anti-mGluR6 (rabbit polyclonal, 1:400; Nomura et al., 1994). A Texas Red-conjugated, donkey anti-mouse IgG or anti-rabbit IgG secondary antibody (Jackson ImmunoResearch) was used for indirect immunodetection. Nuclear staining was performed using 4′,6-diamidine-2-phenylindole-dihydrochloride (DAPI) at a final concentration of 0.0005%. Slides were scored blind to genotype of dissociated tissue on Zeiss Axiophot fluorescent microscope.

Immunohistochemistry on retinal sections was performed as described above for dissociated cells except that FITC-conjugated secondary antibodies (Jackson ImmunoResearch) were used. Tissue sections were treated with 400 μg/ml of RNase A (Sigma) prior to Propidium Iodide (1 μg/ml; Sigma) staining in place of DAPI to label nuclei. Tissue sections stained for fluorescence were viewed on a Leica TCS-NT confocal microscope.

Construction and generation of replication-incompetent retroviral vectors

The viral construct used as parent and control vector was pLIA (Bao and Cepko, 1997). To obtain the full-length coding cDNA of *neuroD*, an N-terminal coding fragment of *neuroD* (encoding amino acids 1-84) was amplified by PCR from mouse genomic DNA. The PCR-amplified N-terminal fragment was digested with *Tth*III1 and ligated with the remaining 3′ fragment of *neuroD* cDNA from Lee et al. (1995) at the *Tth*III1 site to make a full-coding cDNA. This full coding cDNA was blunt-ended and ligated into the *Sna*B1 site of LIA to make the LIA-NeuroD construct.

To generate virus, the proviral vector plasmids were transfected along with a helper plasmid, Psi$^-$ ecotropic helper, into a subline of 293T cells (Dr Martine Roussel, St Jude Children's Research Hospital, Memphis), utilizing high-efficiency transfection with calcium phosphate-DNA precipitation formed in N,N-bis(2-hydroxyethyl)-2-aminoethanesulfonic acid (BES) buffer (Cepko and Pear, 1997). Supernatant was collected every 6-8 hours, starting at 24 hours post-transfection, and was concentrated and titered as described previously (Cepko and Pear, 1997).

In vivo viral injection and clonal analysis

In vivo injections of retrovirus into developing rat retinae were performed at postnatal day (P) 0, P4 and P7, and clonal analysis was performed as described previously (Turner and Cepko, 1987; Fields-Berry et al., 1992). Optimal titer for clonal analysis was 1.0-2.0×10^7 cfu/ml, and virus was diluted accordingly with DMEM (Life Technologies, Gaithersburg, MD) containing 10% fetal calf serum (Life Technologies). Infected retinae were dissected after 3 weeks, fixed in 4% paraformaldehyde overnight at 4°C, and stained as whole mounts for alkaline phosphatase activity according to Cepko et al. (1998). Retinae were cryoembedded and serially sectioned at 20 μm to visualize infected clones. The cellular composition of each clone (lineally related cells forming radial clusters) was determined through reconstruction of camera lucida drawings or photographs taken with a digital camera (Sony, DKC-5000). Criteria used to identify cell types in clones have been described previously (Turner and Cepko, 1987; Fields-Berry et al., 1992). Neonatal rat littermates were injected in vivo with either LIA or LIA-NeuroD. In most experiments, three trials (i.e. three separate litters) were injected with control and experimental virus.

TUNEL assay

The fluorescein apoptosis detection system (Promega) was used according to the suppliers' instructions. Tissue sections were stained with Propidium Iodide to label nucleic acid, forgoing RNase treatment, and viewed using confocal microscopy.

Statistical methods

In order to evaluate differences between control and experimental values for statistical significance, one of two tests was applied. The two-sample *t*-test for independent samples with unequal variances (Satterthwaite's Method) was utilized for measurements based on continuous data (i.e. average clone size). The two-sample test for binomial proportions was used for measurements based on categorical data (i.e. percentage of one-cell clones).

RESULTS

Expression of *neuroD* in the developing and adult rodent retina

The pattern of *neuroD* gene expression was examined in the developing and adult rat retina by in situ hybridization. *neuroD* exhibited a dynamic gene expression pattern spatially and temporally during development. On embryonic day 13 (E13), despite strong staining elsewhere in the CNS (data not shown), few, faintly expressing retinal cells were detected in the central retina (Fig. 1A). No signal was detected in the ganglion cell layer (GCL) at this stage. Strong *neuroD* expression was first detected at E17, the period of peak amacrine cell genesis (M. LaVail, unpublished data) (Fig. 1B). Expression was detected in a subset of cells along the scleral aspect of the developing neural retina from centre to periphery, where proliferating cells undergo the

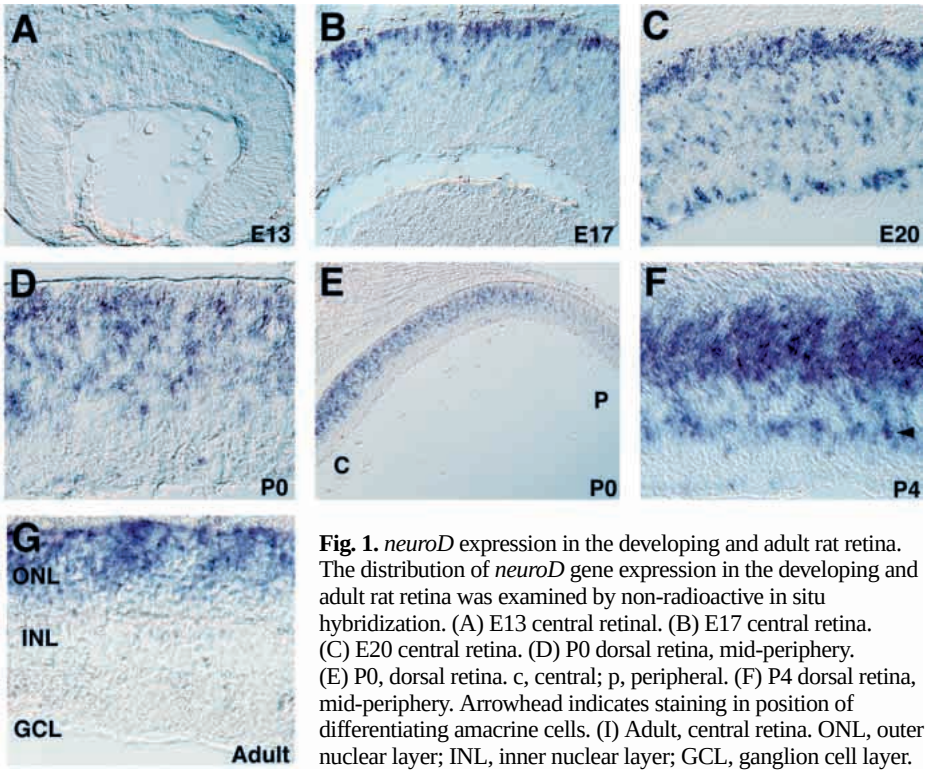

Fig. 1. *neuroD* expression in the developing and adult rat retina. The distribution of *neuroD* gene expression in the developing and adult rat retina was examined by non-radioactive in situ hybridization. (A) E13 central retinal. (B) E17 central retina. (C) E20 central retina. (D) P0 dorsal retina, mid-periphery. (E) P0, dorsal retina. c, central; p, peripheral. (F) P4 dorsal retina, mid-periphery. Arrowhead indicates staining in position of differentiating amacrine cells. (I) Adult, central retina. ONL, outer nuclear layer; INL, inner nuclear layer; GCL, ganglion cell layer.

M phase of the cell cycle and where differentiating cone photoreceptors are found. At E17, no signal was detectable in the GCL. At E20, during peak amacrine cell differentiation, robust *neuroD* expression was detected in a subset of retinal cells across the entire width of the retina, centre to periphery (Fig. 1C). A band of *neuroD* expressing cells was observed along the scleral aspect of the developing retina while punctate *neuroD* staining was observed in the middle part of the developing retina. In addition, approximately 30-40% of the cells residing in the GCL (corresponding to expression in either ganglion cells or displaced amacrine cells) displayed strong *neuroD* expression.

At postnatal day 0 (P0), *neuroD* transcripts were detected across the outer half of the retina where undifferentiated cells and prospective photoreceptors are found (Fig. 1D). The expression pattern was also found in a central to peripheral gradient (Fig. 1E). *neuroD* expressing cells were most abundant in the central retina, extending across the entire differentiating ONL, and less abundant in the periphery (Fig. 1E). This spatial pattern of expression mimicked patterns of expression previously reported for several photoreceptor-specific genes, such as rhodopsin (Treisman et al., 1988). The timing of *neuroD* expression in developing photoreceptors, however, preceded the expression of other photoreceptor-specific genes, with the exception of *Crx*, which was similarly expressed both spatially and temporally (Chen et al., 1997; Furukawa et al., 1997, and data not shown). At P4, in addition to strong expression in regions of undifferentiated cells and presumptive photoreceptors, *neuroD* expression was detectable in cells in the inner aspect of the prospective inner nuclear layer (INL), corresponding to differentiating amacrine cells (Fig. 1F). *neuroD* expression was maintained at low levels in the mature retina. In the adult, *neuroD* was expressed predominantly in the ONL, and in the central region of the retina, only in outer photoreceptors (Fig. 1G).

neuroD expression in the mouse retina was examined utilizing a mouse line that was heterozygous for a *lacZ* transgene targeted into the *neuroD* locus, thereby reporting *neuroD* gene transcription (see Materials and methods and below). The expression of *lacZ* during development was highly similar to the expression pattern described above for the rat retina (Fig. 2A-C). In the adult, *neuroD* expression was observed in an interesting central-to-peripheral gradient (Fig. 2D). In the central retina, *neuroD* was observed only in the outermost photoreceptor cells in the ONL (Fig. 2E), while in the peripheral retina expression was found in all photoreceptors (Fig. 2F). In addition, in the most peripheral aspect of the adult mouse retina, β-galactosidase staining was apparent in a small subset of INL and GCL cells in addition to photoreceptors (Fig. 2F).

NeuroD regulates the neuron/glia decision in postnatal retinal development

To investigate the role played by NeuroD in rodent retinal development, we examined the developing retina of NeuroD-null mice in which the entire coding region of the *neuroD* gene was replaced by the *lacZ* gene by homologous recombination (J. E. Lee et al., unpublished). Absence of *neuroD* RNA expression in NeuroD-null mice was confirmed by in situ hybridization (data not shown). NeuroD-null mice are indistinguishable from their littermates at birth, but become severely hyperglycemic and die within 5 days after birth (Naya et al., 1997).

Glial differentiation is enhanced in *neuroD* mutant explants

Retroviral lineage analysis has demonstrated that a common progenitor for neurons and glia persists in the postnatal retina in rodents, and that multiple neuronal cell types including rod photoreceptors, bipolar and amacrine interneurons also share common progenitors in postnatal development (Turner and Cepko, 1987; Turner et al., 1990). To examine the role of NeuroD in postnatal retinal development, retinal explant cultures using tissue derived from NeuroD-mutant mice were initiated at P0 (prior to onset of hyperglycemia). Our laboratory and others have demonstrated that the levels and kinetics of differentiation observed in vivo are maintained in explant cultures (Tomita et al., 1996a; Ezzeddine et al., 1997). Retinal differentiation in explants was examined using immunohistochemistry after cell fate determination and differentiation were completed. After 12 days in vitro (DIV), all of the neurons examined (photoreceptors, amacrines and bipolars) had formed in the NeuroD-null retinae. However, the relative levels of these neurons were altered in *neuroD* mutants compared to controls and the number of glia was significantly increased.

Retinal explants (wild type and mutant) formed the three

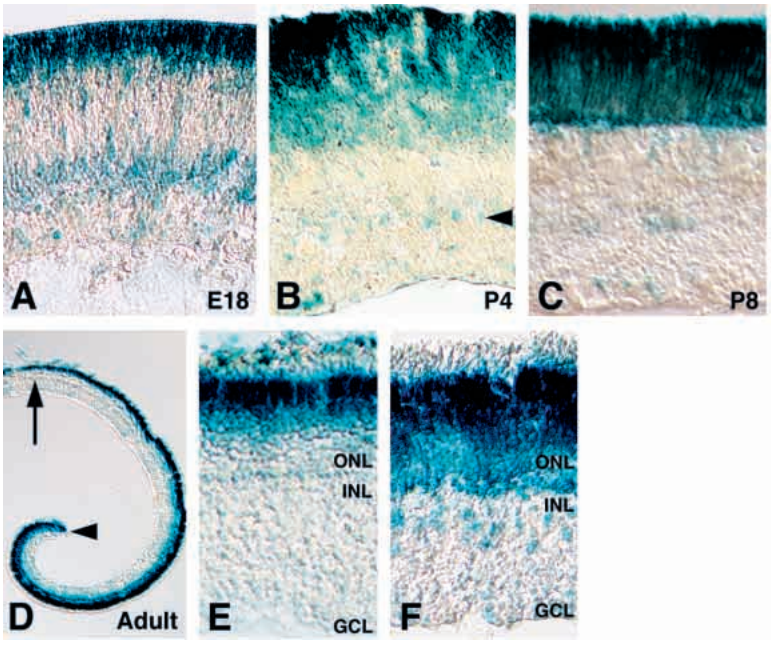

Fig. 2. *neuroD* expression in the developing and adult mouse retina. The distribution of *neuroD* gene expression in the developing and adult mouse retina was examined by X-gal staining in mice heterozygous for a *neuroD* knock-out/lacZ -knock-in locus (see Materials and methods). (A) E18 central retina. (B) P4 dorsal retina, mid-periphery. Strong *neuroD* expression was found across the differentiating photoreceptor layer, as well as in a subset of differentiating amacrine cells (arrowhead). (C) P8 dorsal retina, mid-periphery. (D) Adult, dorsal retina. β-galactosidase staining was detected in outer photoreceptors in the central retina (arrow; see also E) and in all photoreceptors in the peripheral retina (arrowhead; see also F). (E) Adult, central retina. (F) Adult, dorsal peripheral retina.

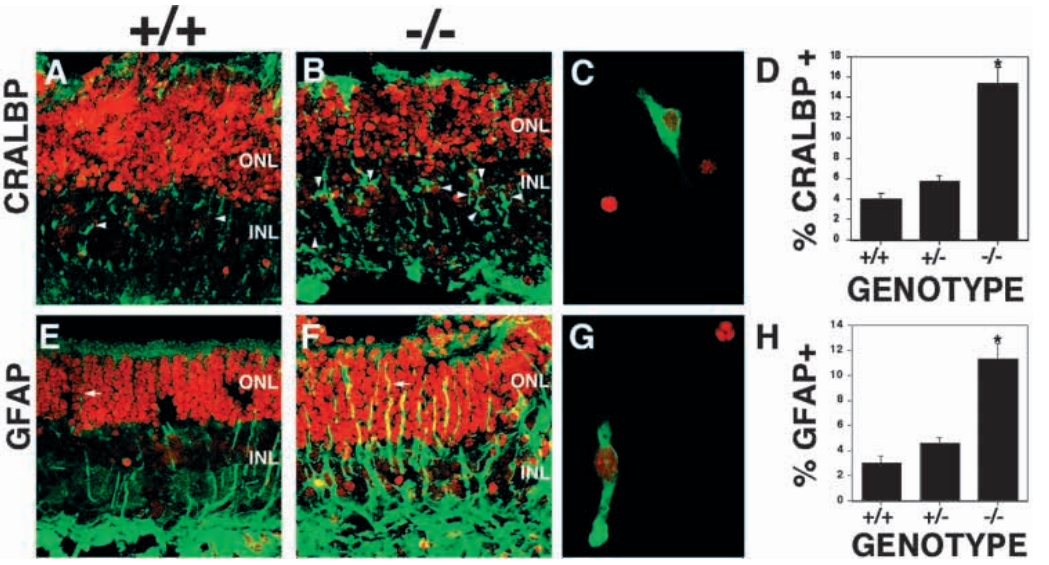

Fig. 3. Glial differentiation is enhanced in NeuroD null retinal explants. Retinal explant culture was initiated at P0. After 12 DIV, retinal sections (A-B and E-F) or dissociated explants (C,G) were stained using anti-CRALBP antibodies or anti-GFAP antibodies to identify Müller glia. Immunoreactivity is shown in green and yellow and nuclear staining in red. Arrowheads in A and B indicate examples of Müller cell bodies. Arrows in E and F indicate representative Müller processes. Examples of CRALBP+ (C) or GFAP+ (G) cells are shown after dissociation of explants. The percentage of Müller cells was measured for each genotype by staining dissociated cells using anti-CRALBP (D) or anti-GFAP (H) antibodies. For both markers, explants were studied from 6 different litters; n=12 explants for the –/– genotype, n=19 explants for the +/+ genotype and n=24 explants for the +/– genotype. The range of increase in glia across experiments was 2.65- to 8.6-fold increase in NeuroD-null tissue over the control for anti-GFAP, and 1.69- to 3.7-fold increase in mutant tissue over the control for anti-CRALBP. *Change compared to control is statistically significant, P<0.001, two-sample t-test for independent samples with unequal variances (Satterthwaite's Method).

cellular layers of the retina after 12 DIV. Using two antibodies raised against different antigens expressed by Müller glia, a higher Müller cell density was consistently observed in NeuroD-null retinae. The anti-cellular retinaldehyde binding protein (CRALBP) antibody, which stains processes and the Müller cell soma located in the INL, showed a greater number of Müller cell bodies in the INL of NeuroD-null retinae (Fig. 3A,B; arrowheads indicate examples of cell bodies). To facilitate quantification of Müller cells, explants were dissociated and stained (Fig. 3C). Consistent with the section staining, CRALBP+ cells were found to increase three to fourfold on average in NeuroD-null explants compared to wild-type controls (Fig. 3D). In NeuroD-null explants, 15.33±1.66% of retinal cells were CRALBP-positive, compared to 4.04±0.53% in wild-type control explants (P<0.001) (Fig. 3D). The anti-glial fibrillary acidic protein (GFAP) antibodies largely stain the Müller processes, which extend radially through the retina, form the outer limiting membrane and line the inner surface of the fiber layer. NeuroD-null retinae were notable for a greater abundance of GFAP+ processes (Fig. 3E,F). In addition, displaced Müller cell bodies were occasionally observed in the ONL (data not shown). For GFAP, 11.36±1.19% of retinal cells were positive in mutant explants, compared to 3.03±0.53% in wild-type controls (P<0.001) (Fig. 3H). Increases in glial differentiation in NeuroD-null explants over control were found to occur as early as 6 days of culture, as determined by intermediate harvests and staining. For CRALBP, 9.14±0.55% in mutant explants as compared to 5.66±0.28% of cells in wild-type controls were marker positive at 6 DIV.

To examine the possibility that increases in the percentages of Müller cells were due to a differential cell loss of neurons, the number of cells per explant was quantified. Wild-type and mutant retinae were indistinguishable by size at P0 when cultures were initiated (data not shown). On average, the total number of cells recovered from mutant explants was 12.9±11.9% lower than wild-type explants. This difference in cell number per explant is likely due to the cell death of a subset of photoreceptors in culture (see below and Fig. 8), but the magnitude of this death is not large enough to explain the increased percentages of Müller cells observed.

To examine the possibility that increases in glial cell numbers were the result of astrocyte contamination, retinae were examined for the presence of astrocytes prior to the establishment of the explant culture. Astrocytes are found predominantly in or near the optic nerve head at the age dissected and this region was generally removed during dissection (Watanabe and Raff, 1988; Fruttiger et al., 1996). Dissected retinal tissue was tested for contaminating astrocytes by immunohistochemical staining for glial fibrillary acidic protein (GFAP), which would stain primarily astrocytes at this

Table 1. Analysis of proliferation in NeuroD null explant cultures

Genotype	%CRALBP+/total	%BRDU+/total	%BRDU+/CRALBP+
+/+	4.69±1.27	2.33±0.03	18.75±4.38
–/–	12.65±1.53	1.17±0.73	10.20±0.28

Retinae were harvested at P0 and cultured as explants for 8 days. On day 8, BrdU was added to a final concentration of 10 mM and left in the medium for the remainder of the culture period. At 12 DIV, retinal explants were dissociated and double stained using anti-BrdU antibodies and anti-CRALBP antibodies. The CRALBP+ cells as a percentage of total cells, BrdU+ cells as a percentage of total, and doubly positive cells as a percentage of CRALBP+ cells, were scored. Shown are the averages ± s.d. Data were derived from one litter; n=3 explants for +/+ and n=2 for –/–.

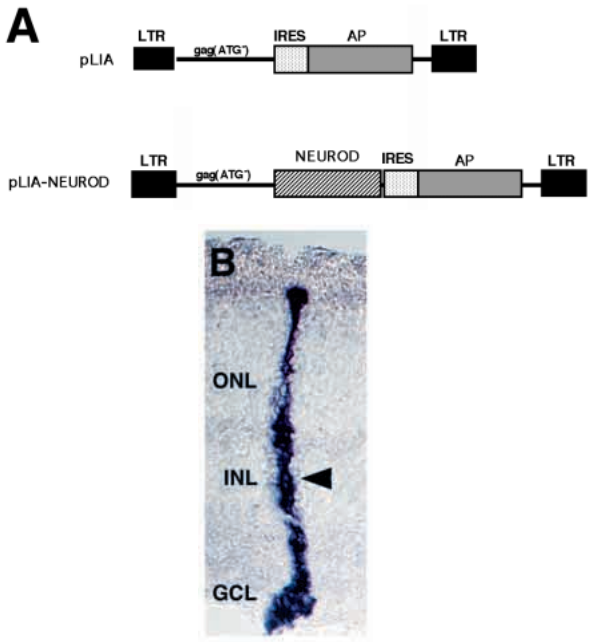

Fig. 4. Retroviral transduction of retinal progenitor cells in vivo. (A) Retroviral vector constructs. The open reading frame for mouse NeuroD was subcloned in front of an internal ribosomal entry site (IRES) in pLIA, found 5′ of the coding sequence for alkaline phosphatase (AP) to generate pLIA-NeuroD. Virus generated using this construct expresses a dicistronic mRNA encoding NeuroD and AP transcribed from the viral LTR promoter. LIA control virus encodes AP alone (see Materials and methods for details). (B) A clone containing a Müller glial cell. The arrowhead indicates the position of cell body. The morphology of retinal clones stained for alkaline phosphatase histochemistry has been previously described in Fields-Berry et al. (1992).

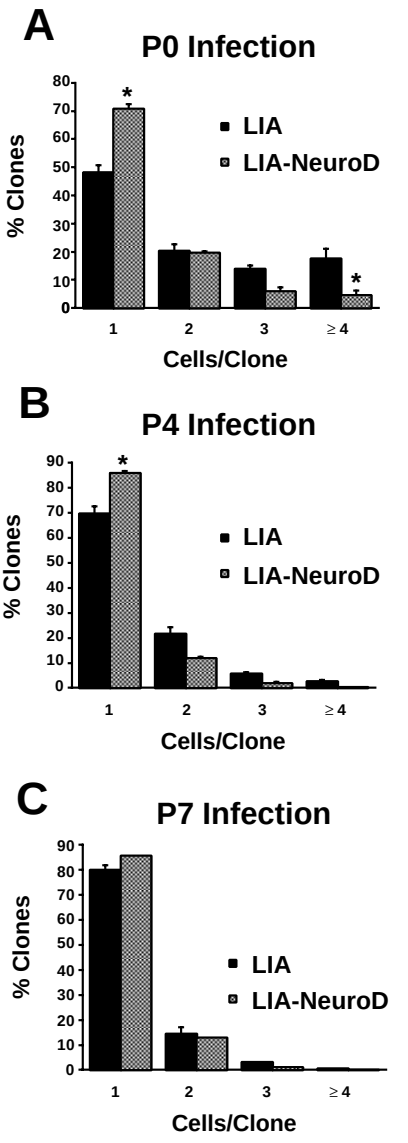

Fig. 5. Forced *neuroD* expression reduces clone size in vivo. The distribution of clone size is presented for clones resulting from infections at (A) P0, (B) P4 or (C) P7 with LIA-NeuroD or LIA in vivo. The averages of three trials ± s.e.m. are shown, except for P7 where fewer trials were performed. See Table 2 legend for details about number of trials per infection timepoint and number of clones scored per trial. *Change compared to control is statistically significant, $P<0.001$, two-sample test for binomial proportions.

stage. Müller glia are born largely after P0 (Young, 1985) in the mouse retina. Less than 0.005% of cells (0/20,000) after dissociation and immunostaining were GFAP$^+$ at P0, thereby indicating that astrocyte contamination was minimal.

To examine the possibility that increases in Müller glia were the result of differential proliferation of Müller cells in culture, proliferation was analyzed in culture using BrdU labelling (Table 1). BrdU was maintained in culture from 8 DIV to 12 DIV. At the end of 12 DIV, 10.20±0.28% of CRABLP+ cells were also BrdU+ in NeuroD-null retinae, as compared to 18.75±4.38% of CRALBP+ cells for wild-type explants. Based on these data, the increase in Müller cells is unlikely to be due to an overproliferation of glia, as approximately 90% of Müller precursors were not mitotic after 8 DIV. As a result of the exclusion of differential cell death of neurons and differential proliferation of glia, the increases in Müller cells observed in the NeuroD-null retinae are likely to be the result of an increase in glial determination at the expense of neuronal determination in the absence of NeuroD in a subset of postnatal retinal progenitors.

Forced *neuroD* expression blocks gliogenesis in vivo

To further examine the function of NeuroD in retinal development, a murine replication-incompetent retrovirus, LIA-NeuroD, coexpressing *neuroD* and a histochemical marker gene, alkaline phosphatase (AP), was constructed. LIA-NeuroD or LIA (encoding AP alone) (Fig. 4A) retroviruses were injected into developing retinae of littermates at P0 in vivo. Mature retinae were harvested 4-6 weeks after infection, processed for AP histochemistry, and the cellular composition of clones (lineally related cells forming radial arrays) was scored after serial reconstruction. The morphology of retinal clones labelled with AP histochemistry has been previously described by Fields-Berry et al. (1992). The developmental fate of a singly infected progenitor or the fates of this cell's progeny (composing a clone) were thereby compared for progenitors transduced in vivo with the *neuroD*-expressing virus or the control virus. Littermates were injected from three separate litters with either LIA-NeuroD or LIA, and approximately 500

clones infected with each virus were analyzed from each retina. The distribution of clones taken from the central and peripheral retina were approximately equivalent for LIA-NeuroD and LIA-infected retinae.

The composition of retinal clones transduced by LIA-NeuroD was significantly altered in several ways relative to the composition of clones transduced by the control LIA virus. First, LIA-NeuroD transduced clones were completely devoid of Müller glial cells. Fig. 4B is an example of a Müller-containing clone. When retinal progenitors were infected at P0 in vivo with LIA control virus, 7.34±0.89% of clones contained at least one Müller glial cell. When transduced with LIA-NeuroD, 0% of resulting clones contained glia (Table 2). No abnormally differentiating glia or neurons were observed in the NeuroD transduced clones in retinae harvested 3 weeks or more post-infection. No difference in unidentifiable cells (0.50±0.09% of total cells for LIA versus 0.13±0.10% for LIA-NeuroD), which are usually unidentifiable due to poor staining of cells, was detected. To examine the possibility that the absence of glia was due to selective cell killing due to *neuroD* expression, intermediate harvests were conducted at 5 and 10 days post-infection. No differentiated glia or abnormally differentiating cells were identified at these time points.

In addition to a loss of glia, clones transduced with *neuroD*-expressing virus exhibited a significant decrease in the number of cells per clone relative to clones transduced with control virus (Fig. 5 and Table 3), suggesting that NeuroD may promote cell cycle withdrawal. This decrease in clone size could not be accounted for by the loss of glia alone as the percentage of cells that were glia in the control was too small a fraction of all cells generated. When retinal progenitors were transduced at P0 with a *neuroD*-expressing virus, the percentage of clones composed of only a single cell was significantly increased. Single-cell clones represented 70.74±1.64% of all LIA-NeuroD clones, as compared to 48.21±2.47% for control LIA clones (P<0.001) (Fig. 5A). Correspondingly, multiple-cell clones were observed less frequently in NeuroD-transduced clones relative to control LIA-transduced clones (Fig. 5A). Overall, the average clone size resulting from infection at P0 with LIA-NeuroD virus was significantly reduced: 1.4±0.1 cells as compared to 2.2±0.1 cells for the control LIA virus (P<0.05) (Table 3).

To rule out the possibility that the loss of glia from clones resulting from transduction with LIA-NeuroD at P0 was an indirect result of forcing cell cycle withdrawal at P0, when relatively few glia are produced during normal development, retinal progenitors were infected at P4 and P7 during peak periods of gliogenesis. At P4, the clone size was only moderately reduced, after infection with LIA-NeuroD relative to control (Fig. 5B and Table 3). At P7, clone size even in LIA-infected retinae was already close to an average of 1.0 cells/clone, so clone size could not be significantly reduced (Table 3). At these peak periods of gliogenesis, clones resulting from transduction of progenitors with LIA-NeuroD virus exhibited a complete absence of glia (Table 2). For control LIA clones, 10.81±0.97% and 11.51±0.40% of clones contained glia after infection at P4 and P7 respectively. Again, no abnormally differentiating glia or neurons were observed in the NeuroD-transduced clones in retinae harvested 3 weeks or more post-infection.

NeuroD overexpression favours amacrine cells and rod photoreceptors, and reduces bipolar cells

To address the question of whether NeuroD differentially

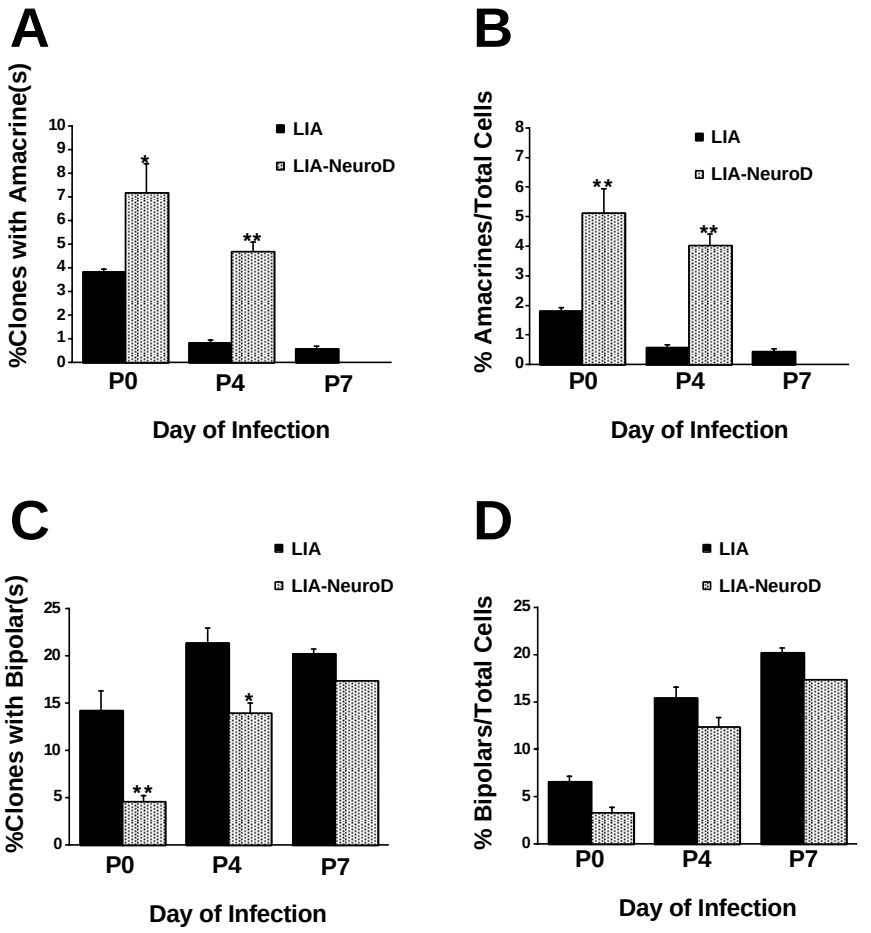

Fig. 6. NeuroD overexpression favours amacrine interneurons over bipolar interneurons in vivo. Transduction of retinal clones with *neuroD*-expressing virus significantly increased the representation of amacrine interneurons (A,B), and decreased the representation of bipolar interneurons (C,D). Shown are the percentages of clones that contain at least one (A) amacrine or (C) bipolar cell after infection at P0, P4 or P7 with LIA-NeuroD or LIA in vivo. Also shown are (B) amacrine or (D) bipolar cells represented as a percentage of the total cells labelled (without regard to clonality). Presented are the averages of three trials ± s.e.m., except for P7 where fewer trials were performed. See Table 2 legend for details about number of trials per infection timepoint and number of clones scored per trial. *Change compared to control is statistically significant, P<0.05, two-sample test for binomial proportions. **Change compared to control is statistically significant, P<0.002, two sample test for binomial proportions.

Table 2. NeuroD blocks glial cell fate in vivo

Day of infection	Virus	Number of clones with glial cell(s) (sum of trials)	Number of clones scored (sum of trials)	% clones with glia (average±s.e.m.)
P0*	LIA	89	1278	7.34±0.89
	LIA-NeuroD	0	1533	0.00±0.00
P4*	LIA	109	1036	10.81±0.97
	LIA-NeuroD	0	1092	0.00±0.00
P7**	LIA	95	813	11.51±0.40
	LIA-NeuroD	0	455	0.00±0.00

The ability to generate clones with glia by progenitor cells transduced by *neuroD*-expressing viruses was examined. Neonatal rat littermates were injected in vivo with LIA-NeuroD or LIA retrovirus at P0, P4 or P7. Mature retinae were harvested at 4-6 weeks of age, and processed for alkaline phosphatase histochemistry. The cellular composition of clones (lineally related cells forming radial clusters) was scored after serial reconstruction (see Materials and methods). Values are averages ± s.e.m.

*Data for P0 and P4 injections represent the sum or average of three trials using separate litters for each trial. Approximately 500 clones were collected from a single retina per trial for LIA or LIA-NeuroD P0 injections. Approximately 300-500 clones were collected from one or two littermate retinae per trial for P4 injections.

**Two trials using separate litters for each trial were performed for the LIA control virus for P7 injections. In trial 1, 508 clones from one retina were scored, and for trial 2, 305 clones were scored from two littermate retinae. Only one trial was performed for the LIA-NeuroD virus at P7, for which 455 clones were collected from a single retina.

Unidentifiable cells, usually due to poor staining, comprised 0.50±0.09% (LIA) versus 0.13±0.10% (LIA-NeuroD), 0.23±0.10% (LIA) versus 0.30±0.14% (LIA-NeuroD), and 0.23±0.13% versus 0.57% (LIA-NeuroD) of all cells at P0, P4 and P7 respectively.

regulates the development of retinal neurons, the composition of retinal neurons in NeuroD-transduced clones and in NeuroD-mutant retinae developing in culture were examined.

In NeuroD-transduced clones, the number of amacrine cells was significantly increased after infection of progenitors at P0 and P4, but not P7 (Fig. 6). The percentage of clones containing at least one amacrine cell was increased nearly twofold from P0-infected progenitors (P<0.05), and nearly sixfold from P4-infected progenitors (P<0.002) (Fig. 6A). A corresponding decrease in bipolar containing clones was observed at these stages (Fig. 6C). Bipolar-containing clones were decreased over threefold for P0-infected progenitors (P<0.001), and by 35% for P4-infected progenitors (P<0.01) (Fig. 6C). Interestingly, the effects on bipolar cells became more moderate with increased developmental stage. Correspondingly, amacrine cells were not increased at the P7 infection timepoint (Fig. 6A,B).

To approximate cells undergoing their terminal mitosis at the time of infection and thereby attempt to separate effects on cell fate from effects on cell proliferation, single-cell clones were examined for their neuronal composition (Table 4). (Note the retrovirus integrates into only one genome during M phase, and is thus passed to only one daughter cell; Roe et al., 1993.) After infection at P0 with LIA-NeuroD, 4.56±0.98% of one-cell clones were composed of a single amacrine cell, as compared to 1.36±0.16% for LIA-infected clones (P<0.01). Single bipolar clones showed complementary decreases (Table 4). This trend was maintained for P4-infected progenitors.

Table 3. Forced *neuroD* expression in retinal progenitors reduces clone size in vivo

	Day of infection	LIA	LIA-NeuroD
Cells/clone	P0	2.2±0.1	1.4±0.1*
	P4	1.4±0.0	1.2±0
	P7	1.3±0	1.2
Largest clone	P0	11.0±1.6	5.7±0.7
	P4	5.3±0.3	4.0±0.5
	P7	5.0±0.6	4.0

Clone size resulting from transduction of progenitor cells with either LIA-NeuroD or LIA control virus was examined. Neonatal rat littermates were injected in vivo with either LIA-NeuroD or LIA retrovirus at P0, P4 or P7. Mature retinae were harvested at 4-6 weeks of age, and processed for alkaline phosphatase histochemistry. The number of cells per clone (lineally related cells forming radial clusters) was scored after serial reconstruction (see Materials and methods). Values are the average of three trials ± s.e.m., except for P7 where fewer trials were performed. See Table 2 for details of number of trials and clones scored per trial.

*Change compared to control is statistically significant, P<0.05, two-sample t-test for independent samples with unequal variances (Satterthwaite's Method).

The representation of rod photoreceptors was moderately increased in clones transduced by LIA-NeuroD. While the percentage of clones containing at least one rod after P0 infections was not altered (96.28±0.48% for LIA versus 95.45±0.48% for LIA-NeuroD), such clones showed small increases after P4 (83.61±1.18% for LIA versus 88.01±1.30% for LIA-NeuroD) and P7 infections (79.63±1.27% for LIA versus 86.81% for LIA-NeuroD). The percentages of clones containing exclusively rods was also moderately increased (for LIA and LIA-NeuroD respectively, 76.81±4.43% versus 88.35±1.76% at P0, 68.80±3.01% versus 81.41±2.48% at P4, and 67.99±1.85% versus 81.98% at P7), as was the representation of rods as a percentage of total cells (data not shown) across all infection time points.

Again to approximate clones undergoing their terminal M phase at the time of infection, single-cell clones were examined. The representation of one-rod clones as a percentage of all single-cell clones was not significantly altered after P0 infections: 92.83±1.59% (LIA) versus 93.73±0.66% (LIA-NeuroD). However, these clones showed moderate increases at P4 and P7 infections: 78.78±1.50% (LIA) versus 86.39±0.69% (LIA-NeuroD) at P4 (P<0.02), and 74.73±0.01% versus 85.89% (LIA-NeuroD) at P7 (P<0.01) (Table 4).

Increased bipolar differentiation in a dose-dependent fashion in *neuroD* mutant retinae

Neuronal differentiation was examined in NeuroD-null retinae in vivo and in vitro, using cell-type specific markers. Amacrine differentiation appeared delayed in NeuroD-null retinae.

Table 4. Single-neuron clones transduced by LIA-NeuroD or LIA in vivo

Day of infection	Cell type in single-cell clone	% clones with given cell type *LIA*	% clones with given cell type *LIA-NeuroD*
P0[1]	Amacrine	1.36±0.16	4.56±0.98**
	Bipolar	4.41±0.93	1.71±0.82
	Rod	92.38±1.60	93.73±0.66
P4[2]	Amacrine	0.17±0.23	3.0±0.39**
	Bipolar	14.68±1.05	10.37±0.59
	Rod	78.78±1.50	86.39±0.69*
P7[3]	Amacrine	0.45±0.03	0
	Bipolar	15.26±1.01	13.85
	Rod	74.73±0.01	85.89**

The representation of rod photoreceptors, amacrine and bipolar interneurons in single-cell clones infected at P0, P4 or P7 with LIA-NeuroD or LIA in vivo was examined. Values are averages ± s.e.m.

[1]Data for P0 injections represent the average of three trials using separate litters for each trial. The number of single-cell clones was 249 (LIA) and 354 (LIA-NeuroD), 114 (LIA) and 351 (LIA-NeuroD), and 266 (LIA) and 379 (LIA-NeuroD) for trials 1, 2 and 3, respectively. Each trial was collected from a single retina.

[2]Data for P4 injections represent the average of three trials using using separate litters for each trial. The number of single-cell clones was 202 (LIA) and 233 (LIA-NeuroD), 337 (LIA) and 446 (LIA-NeuroD), and 189 (LIA) and 263 (LIA-NeuroD) for trials 1, 2 and 3, respectively. Each trial was collected from one or two littermate retinae.

[3]P7 data from two trials of 392 (from one retina in litter 1) and 253 (from two retinae in litter 2) single-cell clones collected for LIA. For LIA-NeuroD, a single trial containing 390 single-cell clones from a single retina was performed.

*Change compared to control is statistically significant, $P<0.02$, two-sample test for binomial proportions.

**Change compared to control is statistically significant, $P<0.01$, two-sample test for binomial proportions.

Amacrine cell differentiation was examined by staining freshly dissociated P0 retinae using the antibody VC1.1. The percentage of VC1.1+ cells demonstrated small but statistically significant reductions in the NeuroD-null retinae (6.89±0.37% of retinal cells) relative to wild-type controls (9.68±0.67%) ($P<0.05$) (Fig. 7A). Using an anti-recoverin antibody, which stains largely cones at P0, no reduction in staining was noted in the NeuroD-null retina relative to wild-type controls (Fig. 7B). Thus, the initial steps of cone photoreceptor differentiation appeared unaffected by loss of NeuroD at P0. In addition, no differences in the levels of rod photoreceptor differentiation (using anti-rhodopsin staining) or Müller glia differentiation (using anti-CRALBP staining) were detected at P0. Both of these cell types represented less than 1% of all cells at this stage of development (data not shown).

Using two antibodies raised against antigens expressed in subsets of amacrine cells, GAT-1 (Fig. 7C) and VC1.1 (Fig. 7D), the number of amacrine cells appeared to reach normal levels after 12 DIV in the absence of NeuroD. β-galactosidase+ amacrine cells in P12 NeuroD-null explants (representing cells expressing the mutated *neuroD* gene) were evident and found to extend processes into the INL after development in vitro (data not shown). Based on these results, amacrine cell differentiation appears delayed but may not be reduced overall in the absence of NeuroD.

The kinetics of rhodopsin expression in the explant cultures (quantifying Rho4D2+ cells on intermediate harvests) was largely unaltered in the absence of NeuroD (data not shown), while the final number of rods after 12 DIV was moderately reduced (60.66±4.22% of NeuroD-null retinal cells were Rho4D2+, as compared to 70.47±1.24% for control retinal cells; Fig. 7E). Using anti-β-galactosidase antibodies to identify developing photoreceptors expressing the mutated *neuroD* gene, rhodopsin expression was demonstrated directly on these NeuroD-null cells (Fig. 7F). In addition, another rod and cone protein, recoverin, was found to be expressed in differentiated rods in NeuroD-null retinae (data not shown). Because photoreceptor outer segments generally do not develop in vitro, we were unable to study outer segment formation and photoreceptor physiology in the absence of NeuroD. Photoreceptor activity evaluated by ERG analysis in vivo was indistinguishable between *neuroD* mutant heterozygotes and wild-type littermates after 13 months of age (T. Li, E. M. Morrow and C. L. Cepko, data not shown).

Bipolar cell differentiation was assessed using anti-mGluR6 antibodies, which stain a subset of bipolar cells (Fig. 7G). Interestingly, the number of these bipolar cells was increased in a dose-dependent fashion in the absence of NeuroD. In wild-type control retinae, 3.64±0.41% of retinal cells expressed mGluR6, as compared to 6.62±0.64 for heterozygous mutant explants ($P<0.001$) and 9.06±1.01% in NeuroD-null explants ($P<0.001$).

Finally, to explore the possibility of neuronal cell death in the NeuroD-null retinae, P0 retinae and explants cultured for 6 or 12 days were examined for apoptotic cells using a TUNEL assay. Little apoptosis was observed in either NeuroD-null or wild-type retinae prior to P12 (Fig. 8A-D). A subset of photoreceptors in the NeuroD-null explants underwent apoptosis by P12. Less apoptosis was observed in the ONL of wild-type explants at this stage (Fig. 8E-F). Many of the apoptotic photoreceptors were rhodopsin+ as determined by double staining (data not shown), indicating that, at least in some cases, apoptosis followed rhodopsin synthesis in the development of these cells.

DISCUSSION

Development of neural tissues is a complex process involving cell proliferation, cell type specification and differentiation, and cell death. To begin to understand the function of the bHLH transcription factor NeuroD in the development of the neural retina, we have conducted both loss-of-function and gain-of-function analyses in this tissue.

Our data demonstrate that NeuroD plays a variety of roles in retinal development. Consistent with the described gene expression pattern (see below), NeuroD (1) participates in the neuron/glia cell fate decision, (2) regulates interneuron differentiation, favouring amacrine differentiation over bipolar differentiation, and (3) appears to be necessary for the survival of a subset of photoreceptors. A summary of our results is presented in Fig. 9.

neuroD expression is predominantly in developing amacrines, and in developing and mature photoreceptors

The expression of *neuroD* was examined by two independent methods in rat and mouse. Despite differences in experimental approach, these two methods provided a similar picture of the dynamic expression of *neuroD*. Overall, *neuroD* was expressed predominantly in undetermined retinal cells, and in developing amacrine interneurons and photoreceptors. Expression appeared to be absent from a subset of developing INL cells late in retinal development, likely corresponding to differentiating bipolar interneurons and Müller glia. In addition to our analysis in rat and mouse, *neuroD* expression in the retina has been studied in chick, *Xenopus*, monkey and human (Lee et al., 1995; Acharya et al., 1997; Roztocil et al., 1997; Perron et al., 1998). Where examined during development, *neuroD* expression is consistently reported in developing photoreceptors, although clearly not only in developing photoreceptors. Because cell genesis is protracted in rodent, we have been able to identify more clearly the expression in developing amacrine cells and photoreceptors.

In the mature retina, *neuroD* expression is maintained in terminally differentiated photoreceptors in all species examined (Figs 1G and 2D-F; Acharya et al., 1997; Roztocil et al., 1997; Perron et al., 1998). At present, NeuroD and Crx (Chen et al., 1997; Furukawa et al., 1997) are the only known transcription factors expressed predominantly in photoreceptors in the mature retina. Currently, the expression of *neuroD* and *Crx* are also the earliest known molecular events in the development of photoreceptors in rodent.

In rodent retinal development, at least four positive-acting bHLH genes are expressed: *Neurogenin2/Math4A* (Gradwohl

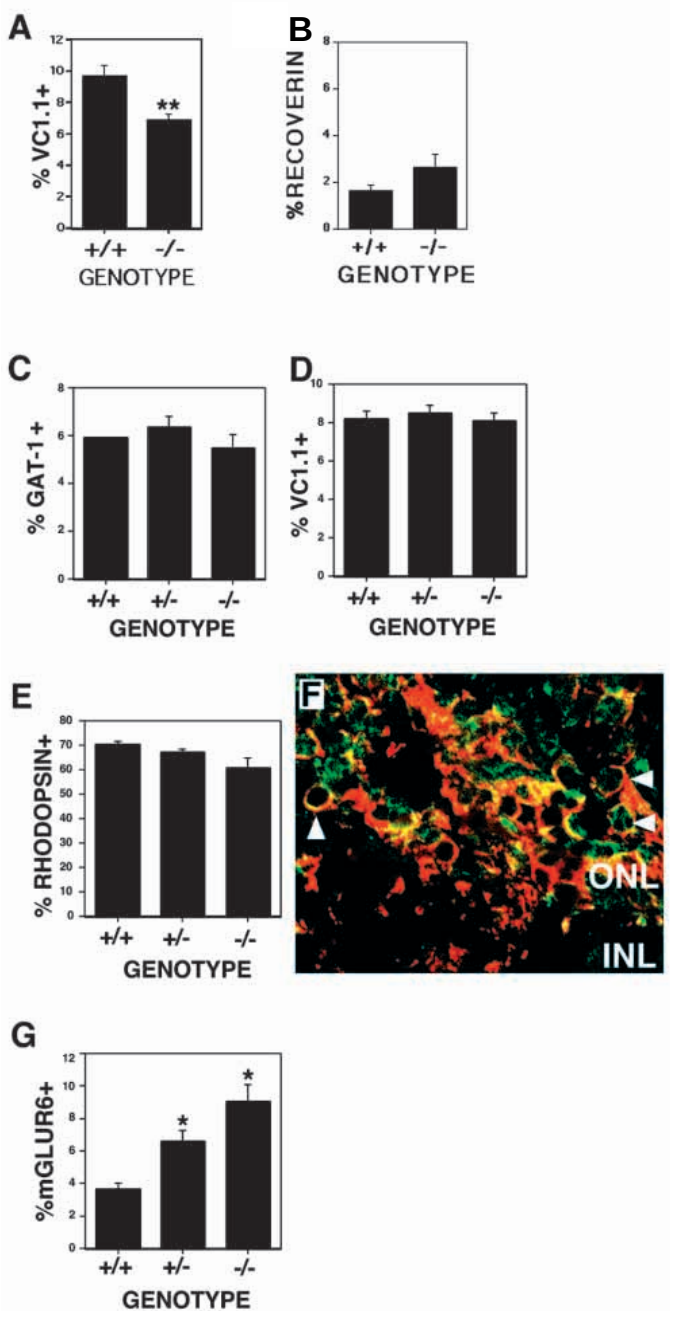

Fig. 7. Neuronal development in NeuroD-null retinae. Retinae from *neuroD* mutant mice were analyzed for neuronal differentiation using cell type specific markers. In (A,B) the percentage of retinal neurons in P0 freshly dissociated retinae was quantified using cell-type specific markers. Amacrine cells (A) VC1.1, or cone photoreceptors (B), anti-recoverin. No differences in the levels of rod photoreceptor differentiation (using anti-rhodopsin staining) or Müller glia differentiation (using anti-CRALBP staining) were detected. Both of these cell types represented less than 1% of all cells at this stage of development (data not shown). In (C-G) retinal explant culture was initiated at P0 and cultures were maintained for 12 DIV. The percentage in explants of the different retinal cell types was quantified for each genotype by staining dissociated cells using cell-type specific markers. Amacrine interneurons: (C) with anti-GAT-1 antibodies or (D) with VC1.1. (E) Rod photoreceptors, anti-rhodopsin antibodies. (F) Rhodopsin expression in retinal cells expressing the mutated NeuroD-allele was confirmed directly by performing double immunohistochemistry using anti-β-galactosidase antibodies to detect expression of the mutant *neuroD* gene (green) and Rho4D2 (red) to detect rhodopsin protein. Arrowheads mark examples of double-positive cells. (G) Bipolar interneurons, anti-mGluR6-antibodies. For VC1.1 and recoverin markers at P0, data were collected from one litter, n=4 explants for the –/– genotype and n=3 for the +/+ genotype. For the amacrine cell markers after 12 DIV, data were collected from one litter; n=3 explants for the –/– genotype, n=4 explants for the +/+ genotype, and n=3 explants for the +/– genotype. For anti-rhodopsin staining, data were collected from 3 separate litters; n=5 explants for the –/– genotype, n=13 explants for the +/+ genotype, and n=8 explants for the +/– genotype. For anti-mGLUR6 staining, data were collected from 3 separate litters; n=10 explants for the –/– genotype, n=17 explants for the +/+ genotype, and n=15 explants for the +/– genotype. *Change compared to control is statistically significant, P<0.001, two-sample t-test for independent samples with unequal variances (Satterthwaite's Method). **Change compared to control is statistically significant, P<0.05, two sample t-test for independent samples with unequal variances (Satterthwaite's Method).

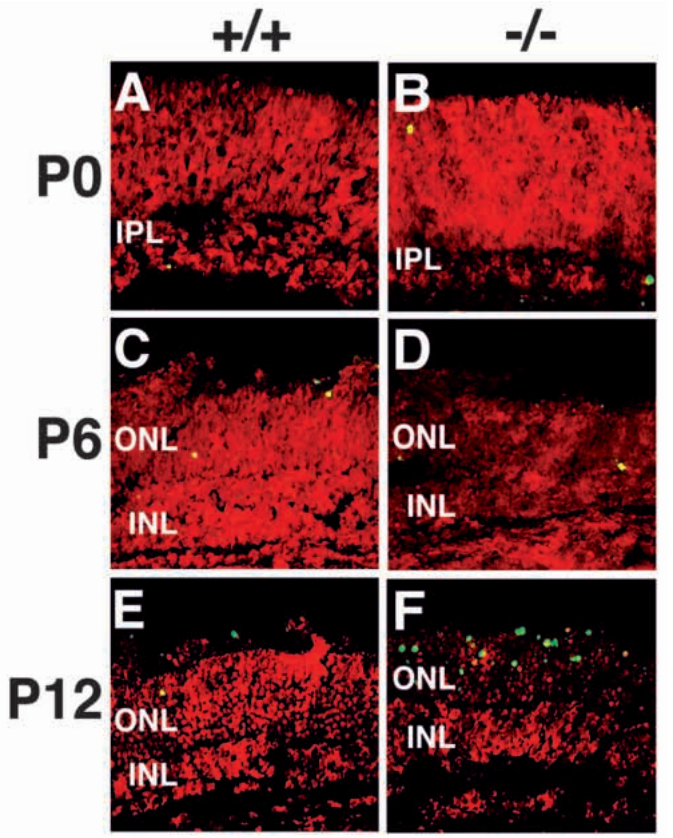

Fig. 8. Apoptosis in NeuroD-null retinal explants. Retinae at P0 (A,B) or retinal explant cultures initiated at P0 and cultured for 6 days (C,D) or 12 days (E,F). Wild-type retinae (A,C,E) and NeuroD-null retinae (B,D,F). Shown are cells undergoing apoptosis using a TUNEL assay (green/yellow). Nuclei are visualized in red using Propidium Iodide staining.

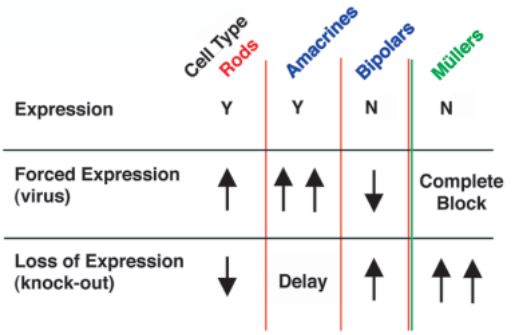

Fig. 9. Summary of expression, loss-of-function, and gain-of-function analyses of *neuroD* in postnatal retinal development. A model for NeuroD function is presented, outlining results from expression, forced expression using retrovirus, and loss of expression using NeuroD-null tissue. Rod photoreceptors (red), interneurons (blue) and glial cells (green). *neuroD* is expressed (Y) in regions of undetermined retinal progenitors, developing rods and amacrine interneurons. It is not expressed (N) in regions of developing bipolars and Müller glia. Arrows indicate the direction of change with perturbation of *neuroD* expression. For virus, arrows indicate the direction of change in percentages of clones containing the given cell type. For knock-out, arrows indicate the direction of change in percentages of retinal cells expressing cell-type specific markers at the end of retinal development. Amacrine differentiation in NeuroD-null tissue appeared delayed, but not decreased overall. A complete loss of Müller cells was observed after transduction with *neuroD*-expressing retroviruses. One arrow indicates changes of threefold or less. Two arrows indicate changes of greater than threefold.

et al., 1996; Sommer et al., 1996), *Mash1*, *ATH-3* and *neuroD*. In postnatal retinal development, *Mash1* expression becomes restricted to developing bipolar cells and Müller glia (Guillemot et al., 1993; Jasoni and Reh, 1996), whereas, as we show here, *neuroD* becomes excluded from these cells. In addition, expression of *ATH-3* and *neuroD* becomes restricted to the INL and ONL, respectively, in the postnatal retina, where their expression is maintained (Takebayashi et al., 1997). A similar complementarity between *neuroD* and *NeuroM* (chick homolog of *ATH-3*) is found in the chick retina late in development (Roztocil et al., 1997). A complete characterization of the spatial and temporal expression of all retinal bHLH proteins relative to each other and the cell cycle would benefit our understanding of the potential function of these molecules in neuronal specification.

NeuroD regulates neuron versus glial cell fate in the developing retina

Forced expression of *neuroD* in common neuron/glial progenitors appeared to hasten cell cycle withdrawal and block gliogenesis in favour of neuronal differentiation. Interestingly, this complete block in gliogenesis is mimicked by other diverse bHLH proteins expressed in the developing nervous system, including MASH1, ATH-3 and Neurogenin2 (E. M. Morrow and C. L. Cepko, unpublished data), but not by transcription factors such as Crx (Furukawa et al., 1997), Rax (T. Furukawa, E. M. Morrow and C. L. Cepko, unpublished), or HES-1 (Tomita et al., 1996a; T. Furukawa and C. L. Cepko, unpublished data). These results are consistent with the interpretation that this subtype of bHLH proteins can promote neuronal determination at the expense of glial determination in the rodent retina and that, at least with respect to blocking the glial cell fate, they are functionally redundant. Similar proposals for a role of these factors in promoting neurogenesis and blocking non-neuronal lineages have been made based on overexpression in *Xenopus* (Zimmerman et al., 1993; Turner and Weintraub, 1994; Ferreiro et al., 1994; Lee et al., 1995; Ma et al., 1996; McCormick et al., 1996; Takebayashi et al., 1997). Alternatively, our overexpression results may suggest that bHLH proteins of this subtype are potently and specifically toxic to glia. While this interpretation cannot be formally excluded, we currently favour the interpretation that these proteins play a critical role in the neuron versus glia decision in late retinal progenitors, based on the results from gene targeting in mouse presented here and elsewhere (Tomita et al., 1996b).

In the present study, we observed that retinal explants derived from NeuroD-null mice demonstrated three- to fourfold increases in Müller glia. This observation is most likely accounted for at the level of cell fate determination, as several alternative developmental mechanisms have been excluded. First, this increased representation of glia is unlikely to be solely due to differential survival of glia over neurons in culture, since differential cell loss accounting for the observed

differences in glia was not observed either by cell counts or using TUNEL assays. In addition, differential proliferation of glia seems unlikely as approximately 90% of glial precursors were postmitotic prior to 8 DIV (Table 1). Instead, one possible interpretation is that in the absence of NeuroD, a subpopulation of neuron/glia progenitors more often chooses the glial cell fate instead of a neuron fate, such as the photoreceptor fate. A similar overproduction of Müller glia was observed in MASH1-null retinae developing in vitro (Tomita et al., 1996b), suggesting that the neuron/glia decision may be cooperatively mediated by these neuronal bHLH transcription factors.

The results presented here on NeuroD are contrary to the current notion of NeuroD as simply a 'differentiation' factor, due to its late expression in development. In the retina a common progenitor for neurons and glia persists late in development (Turner and Cepko, 1987) and significant developmental plasticity remains after the terminal mitosis in differentiating retinal cells (Adler and Hatlee, 1989; Altshuler and Cepko, 1992; Belecky-Adams et al., 1996; Ezzeddine et al., 1997). These qualities may permit bHLH transcription factors that are expressed later in development, such as the NeuroD family, to play roles in neuronal specification as well as differentiation in these tissues.

NeuroD influences neuron-specific development in the rodent retina

Do the bHLH proteins play a role in specifying neurons in proper numbers and ratios in development? Because retinal cells are well-characterized and develop fairly autonomously from other regions of the CNS, the retina offers a powerful model system in which to address the question of neuronal specification. Results in this report suggest that NeuroD plays a role in interneuron specification, neuron differentiation and survival. Further, forced expression of NeuroD resulted in a significant reduction in clone size in vivo, suggesting that NeuroD may also be involved in the mechanisms of cell cycle withdrawal. Evidence for such a role for NeuroD/BETA2 has also been reported recently in the differentiation of enteroendocrine cells (Mutoh et al., 1998). As well, a similar role for MyoD in terminal cell cycle arrest of myoblasts has been proposed (Gu et al., 1993; Halevy et al., 1995). The potential function of NeuroD in the cell cycle needs to be addressed more directly to formally prove the importance of such a role in retinal development.

With respect to the regulation of interneuron class choice by bHLH proteins, we have observed increases in amacrine interneurons and corresponding decreases in bipolar interneurons in clones resulting from transduction of progenitors with NeuroD-expressing viruses. Consistent with the notion that bHLH proteins may have inherent neuron-specifying activity, Kanekar et al. found cell-type specific effects of the bHLH Xath5 in *Xenopus* retinal development (1997). When overexpressed in retinal cells using lipofection, Xath5 promoted the ganglion cell fate, whereas NeuroD did not. We are currently conducting experiments to determine if other bHLH proteins have similar or different effects on cell fate by overexpression. The previous study on Xath5 in the *Xenopus* retina, however, did not determine whether the increase in ganglion cells after Xath5 lipofection was a direct result on cell fate or an indirect result of forcing differentiation at the time of ganglion cell genesis. By contrast, in this study, we have been able to separate effects on cell fate determination from effects on cell cycle by conducting retroviral clonal analyses after infection at various timepoints, and in particular, at late timepoints when the proliferative index is low (such as P4 and P7). For example, the nearly sixfold increase in amacrine-containing clones and the dimunition in bipolar-containing clones after infection at P4 is probably a direct cell fate effect, rather than an indirect result of forcing differentiation at this stage, as amacrine cell genesis is nearly finished at this stage of retinal development and bipolar genesis is peaking (Young et al., 1985; M. LaVail, unpublished data). Interestingly, transduction of P4 progenitors with NeuroD alters the amacrine cell production of these progenitors in such a way that they resemble earlier progenitors (Fig. 6A,B). Different effects from forced expression of *neuroD* at different stages of retinal development (for example increases in amacrine-containing clones after P0 and P4 infections, but not after P7 infections) may be due to temporal changes in the expression of NeuroD-interactor molecules. Finally, beyond a delay in amacrine development, we have failed to find defects in amacrine cell production in NeuroD-null retinae. This may be due to redundancy of bHLH proteins in developing amacrine cells. Alternatively, NeuroD may be essential for an aspect of amacrine cell diversity not tested here, as over 20 different types of amacrine cells exist (MacNeil and Masland, 1998).

Further support to implicate NeuroD in choice of interneuron cell type comes from the studies of NeuroD-null retinae. We observed a dose-dependent overrepresentation of bipolar interneurons in NeuroD-null retinae. Interestingly, the opposite effect on bipolar cells developing in explant cultures was observed in MASH1-null retinae; that is, there was a decrease in bipolar genesis in the absence of MASH1 in vitro (Tomita et al., 1996b), suggesting that NeuroD and MASH-1 may have different roles in specifying bipolar cell fate.

Finally, we have examined the role of NeuroD in the initial stages of photoreceptor development in vivo and in vitro. Based on results from NeuroD-null retinae, NeuroD appears to be non-essential for initiation of expression of photoreceptor proteins, such as rhodopsin and recoverin. A subset of photoreceptors underwent apoptotic cell death after 12 DIV, suggesting that NeuroD may play a role in the survival of these neurons. The observation that *neuroD* expression is maintained in a subset of mature photoreceptors is consistent with this notion. Efforts to rescue viability of the NeuroD-null mice or to generate retina-specific NeuroD-null mutations are currently underway. Advances in this direction will further facilitate investigations of NeuroD function in retinal development.

We wish to thank the Drs R. Molday, J. Hurley, S. Nakanishi, and J. Saari for antibodies; for consultations on statistics, we also thank Dr T. Clemens at Harvard School of Public Health; for technical support, M. Morrow, J. Zitz and B. Wong; for critical reading of the manuscript, Drs M. Belliveau, A. Chen, M. Dyer and C. Tabin; for many helpful discussions and support, the members of the Cepko/Tabin Laboratory. This work was supported by grant # NIH EY08064.

REFERENCES

Acharya, H. R., Dooley, C. M., Thoreson, W. B. and Ahmad, I. (1997). cDNA cloning and expression analysis of NeuroD mRNA in human retina. *Biochem. Biophys. Res. Commun.* **223**, 459-463.

Adler, R. and Hatlee, M. (1989). Plasticity and differentiation of embryonic retinal cells after terminal mitosis. *Science* **243**, 391-393.

Altshuler, D., Turner, D. L. and Cepko, C. L. (1991). Specification of cell type in the vertebrate retina. In *Development of the Visual System* (ed. D. M.-K. Lam and C. J. Shatz), pp. 37-58. Cambridge: MIT Press.

Altshuler, D. and Cepko, C. L. (1992). A temporally regulated, diffusible activity is required for rod photoreceptor development in vitro. *Development* **114**, 947-957.

Bao, Z.-Z. and Cepko, C. L. (1997). The expression and function of *Notch* pathway genes in the developing rat eye. *J. Neurosci.* **17**, 1425-1434.

Belecky-Adams, T., Cook, B. and Adler, R. (1996). Correlations between terminal mitosis and differentiated fate of retinal precursor cells *in vivo* and *in vitro*: analysis with the 'window-labeling' technique. *Dev. Biol.* **178**, 304-315.

Ben-Arie, N., Bellen, H. J., Armstrong, D. L., McCall, A. E., Gordadze, P. R., Guo, Q., Matzuk, M. M. and Zoghbi, H. Y. (1997). Math1 is essential for genesis of cerebellar granule neurons. *Nature* **390**, 169-172.

Campos-Ortega, J. A. (1993). Mechanisms of early neurogenesis in *Drosophila melangaster. J. Neurobiol.* **24,** 1305-1327.

Cepko, C. L., Austin, C. P., Yang, X., Alexiades, M. and Ezzeddine, D. (1996). Cell fate determination in the vertebrate retina. *Proc. Natl. Acad. Sci. USA* **93**, 589-595.

Cepko, C. L. and Pear, W. (1997). Transduction of genes using retrovirus vectors. In *Current Protocols in Molecular Biology* (ed. F. M. Ausubel et al.), pp. 9.9.1-9.12.6. John Wiley & Sons.

Cepko, C. L., Ryder, E., Fekete, D. M. and Bruhn, S. (1998). Detection of β-galactosidase and alkaline phosphatase activities in tissue. In *Cells: A Laboratory Manual Vol. 2 Light Microscopy and Cell Structure* (ed. D. L. Spector, R. D. Goldman and L. A. Leinwand), pp. 393-406. Cold Spring Harbor Laboratory Press, Cold Spring Harbor, NY.

Chen, S., Wang, Q.-L., Nie, A., Sun, H., Lennon, G., Copeland, N. G., Gilbert, D. J., Jenkins, N. A. and Zack, D. J. (1997). Crx, a novel otx-like paired-homeodomain protein, binds to and transactivates photoreceptor cell-specific genes. *Neuron* **19**, 1017-1030.

De Leeuw, A. M., Gaur, V. P., Saari, J. C. and Milam, A. H. (1990). Immunolocalization of cellular retinol-, retinaldehyde- and retinoic acid-binding proteins in rat retina during pre- and postnatal development. *J. Neurocytol.* **2**, 253-264.

Dizhoor, A. M., Ray, S., Kumar, S., Niemi, G., Spencer, M., Brolley, D., Walsh, K. A., Philipov, P. P., Hurley, J. B. and Stryer, L. (1991). Recoverin: a calcium sensitive activator of retinal rod guanylate cyclase. *Science* **251**, 915-918.

Ezzeddine, Z. D., Yang, X., DeChiara, T., Yancopoulos, G. and Cepko, C. L. (1997). Postmitotic cells fated to become rod photoreceptors can be respecified by CNTF treatment of the retina. *Development* **124**, 1055-1067.

Fekete, D., Perez-Miguelsanz, J., Ryder, E. and Cepko, C. (1994). Clonal analysis in the chicken retina reveals tangential dispersion of clonally related cells. *Dev. Biol.* **166**, 666-682.

Ferreiro, B., Kintner, C., Zimmerman, K., Anderson, D. J. and Harris, W. A. (1994). XASH genes promote neurogenesis in *Xenopus* embryos. *Development* **120**, 3649-3655.

Fields-Berry, S. C., Halliday, A. and Cepko, C. L. (1992). A recombinant retrovirus encoding alkaline phosphatase confirms clonal boundary assignment in lineage analysis of murine retina. *Proc. Natl. Acad. Sci. USA **89***, 693-697.

Fode, C., Gradwohl, G., Morin, X., Dierich, A., LeMeur, M., Goridis, C. and Guillemot, F. (1998). The bHLH protein NEUROGENIN 2 is a determination factor for epibranchial placode-derived sensory neurons. *Neuron* **20**, 483-494.

Fruttiger, M., Calver, A. R., Kruger, W. H., Mudhar, H. S., Michalovich, D., Takakura, N., Nishikawa, S. I. and Richardson, W. D. (1996). PDGF mediates a neuron-astrocyte interaction in the developing retina. *Neuron* **17**, 1117-1131.

Furukawa, T., Morrow, E. M., and Cepko, C. L. (1997). Crx, a novel otx-like homeobox gene shows photoreceptor-specific expression and regulates photoreceptor differentiation. *Cell* **91**, 531-541.

Gradwohl, G., Fode, C. and Guillemot, F. (1996). Restricted expression of a novel murine atonal-related bHLH protein in undifferentiated neural precursors. *Dev. Biol.* **180**, 227-241.

Gu, W., Schneider, J. W., Condorelli, G., Kaushal, S., Mahdavi, V. and Nadal-Ginard, B. (1993). Interaction of myogenic factors and the retinoblastoma protein mediates muscle cell commitment and differentiation. *Cell* **72**, 309-324.

Guillemot, F. and Joyner, A. L. (1993). Dynamic expression of the murine Achaete-Scute homologue *Mash1* in the developing nervous system. *Mech. Dev.* **42**, 171-185.

Guillemot, F., Lo, L. C., Johnson, J. E., Auerbach, A., Anderson, D. J. and Joyner, A. L. (1993). Mammalian achaete-scute homolog 1 is required for the early development of olfactory and autonomic neurons. *Cell* **75**, 463-476.

Halevy, O., Novitch, B. G., Spicer, D. B., Skapek, S. X., Rhee, J., Hannon, G. J., Beach, D. and Lassar, A. R. (1995). Correlation of terminal cell cycle arrest of skeletal muscle with induction of p21 by MyoD. *Science* **267**, 1018-1021.

Harris, W. A. (1997). Cellular diversification in the vertebrate retina. *Curr. Opin. Genet. Dev.* **7**, 651-658.

Holt, C. E., Bertsch, T. W., Ellis, H. M. and Harris, W. A. (1988). Cellular determination in the *Xenopus* retina is independent of lineage and birth date. *Neuron* **1**, 15-26.

Jan, Y. N. and Jan, L. Y. (1993). HLH proteins, fly neurogenesis, and vertebrate myogenesis. *Cell* **75**, 827-830.

Jasoni, C. L. and Reh, T. A. (1996). Temporal and spatial pattern of MASH-1 expression in the developing rat retina demonstrates progenitor cell heterogeneity. *J. Comp. Neurol.* **369**, 319-327.

Johnson, J. E., Birren, S. J. and Anderson, D. J. (1990). Two rat homologues of Drosophila achaete-scute specifically expressed in neuronal precursors. *Nature* **346**, 858-861.

Kageyama, R. and Nakanishi, S. (1997). Helix-loop-helix factors in growth and differentiation of the vertebrate nervous system. *Curr. Opin. Genet. Dev.* **7**, 659-665.

Kanekar, S., Perron, M., Dorsky, R., Harris, W. A., Jan, L. Y., Jan, Y. N. and Vetter, M. L. (1997). Xath5 participates in a network of bHLH genes in the developing Xenopus retina. *Neuron* **19**, 981-994.

Kume, H., Maruyama, K., Tomita, T., Iwatsubo, T., Saido, T. C. and Obata, K. (1996). Molecular cloning of a novel basic helix-loop-helix protein from the rat brain. *Biochem. Biophys. Res. Commun.* **219**, 526-530.

Lee, J. E., Hollenberg, S. M., Snider, L., Turner, D. L., Lipnick, N. and Weintraub, H. (1995). Conversion of Xenopus ectoderm into neurons by NeuroD, a basic helix-loop-helix protein. *Science* **268**, 836-844.

Lee, J. E. (1997). Basic helix-loop-helix genes in neural development. *Curr. Opin. Neurobiol.* **7**, 13-20.

Ma Q., Kintner C. and Anderson D. J. (1996). Identification of neurogenin, a vertebrate neuronal determination gene. *Cell* **87**, 43-52.

Ma Q., Chen Z., del Barco Barrantes I., de la Pompa J. L. and Anderson D. J. (1998). neurogenin1 is essential for the determination of neuronal precursors for proximal cranial sensory ganglia. *Neuron* **20**, 469-482.

MacNeil, M. A. and Masland, R. H. (1998). Extreme diversity among amacrine cells: Implications for function. *Neuron* **20**, 971-982.

McCormick, M. B., Tamimi, R. M., Snider, L., Asakura, A., Bergstrom, D. and Tapscott, S. J. (1996). NeuroD2 and neuroD3: distinct expression patterns and transcriptional activation potentials within the neuroD gene family. *Mol. Cell. Biol.* **16**, 5792-5800.

Molday, R. S. (1989). Monoclonal antibodies to rhodopsin and other proteins of rod outer segments. *Prog. Ret. Res.* **8**, 173-209.

Morrow, E. M., Belliveau, M. J., and Cepko, C. L. (1998). Two phases of rod photoreceptor differentiation during rat retinal development. *J. Neurosci.* **18**, 3738-3748.

Mutoh, H., Naya, F. J., Tsai, M. J. and Leiter, A. L. (1998). The basic helix-loop-helix protein BETA2 interacts with p300 to coordinate differentiation of secretin-expressing enteroendocrine cells. *Genes Dev.* **12**: 820-830.

Naya, F. J., Stellrecht, C. M. and Tsai, M. J. (1995). Tissue-specific regulation of the insulin gene by a novel basic helix-loop-helix transcription factor. *Genes Dev.* **9**, 1009-1019.

Naya, F. J., Huang, H. P., Qiu, Y., Mutoh, H., DeMayo, F. J., Leiter, A. B. and Tsai M. J. (1997). Diabetes, defective pancreatic morphogenesis, and abnormal enteroendocrine differentiation in BETA2/NeuroD-deficient mice. *Genes Dev.* **11**, 2323-2334.

Nomura, A., Shigemoto, R., Nakamura, Y., Okamoto, N., Mizuno, N. and Nakanishi, S. (1994). Developmentally regulated postsynaptic localization of a metabotropic glutamate receptor in rat rod bipolar cells. *Cell* **77**, 361-369.

Perron, M., Kanekar, S., Vetter, M. L. and Harris, W. A. (1998). The genetic sequence of retinal development in the ciliary margin of the Xenopus eye. *Dev. Biol.* **199**, 185-200.

Porcher, C., Swat, W., Rockwell, K., Fujiwara, Y., Alt, F. W. and Orkin, S. H. (1996). The T-cell leukemia oncoprotein SCL/tal-1 is essential for development of all hematopoietic lineages. *Cell* **86**, 47-57.

Riddle, R. D., Johnson, R. L., Laufer, E. and Tabin C. (1993). Sonic hedgehog mediates the polarizing activity of the ZPA. *Cell* **75**, 1401-1416.

Roe, T., Reynolds, T. C., Yu, G., and Brown, P. O. (1993). Integration of murine leukemia virus DNA depends on mitosis. *EMBO J.* **12**, 2099-2108.

Roztocil, T., Matter-Sadzinski, L., Alliod, C., Ballivet, M. and Matter, J. M. (1997). NeuroM, a neural helix-loop-helix transcription factor, defines a new transition stage in neurogenesis. *Development* **124**, 3263-327

Schwab, M. H., Druffel-Augustin, S., Gass, P., Jung, M., Klugmann, M., Bartholoma, A., Rossner, M. J. and Nave K. A. (1998). Neuronal basic helix-loop-helix proteins (NEX, neuroD, NDRF): spatiotemporal expression and targeted disruption of the NEX gene in transgenic mice. *J. Neurosci.* **18**, 1408-1418.

Shimizu, C., Akazawa, C., Nakanishi, S. and Kageyama R. (1995). MATH-2, a mammalian helix-loop-helix factor structurally related to the product of Drosophila proneural gene atonal, is specifically expressed in the nervous system. *Eur. J. Biochem.* **229**, 239-248.

Sommer, L., Ma, Q. and Anderson, D. J. (1996). Neurogenins, a novel family of atonal-related bHLH transcription factors, are putative mammalian neuronal determination genes that reveal progenitor cell heterogeneity in the developing CNS and PNS. *Mol. Cell Neurosci.* **8**, 221-241.

Takebayashi, K., Takahashi, S., Yokota, C., Tsuda, H., Nakanishi, S., Asashima, M. and Kageyama R. (1997). Conversion of ectoderm into a neural fate by ATH-3, a vertebrate basic helix-loop-helix gene homologous to Drosophila proneural gene atonal. *EMBO J.* **16**, 384-395.

Tomita, K., Ishibashi, M., Nakahara, K., Ang, S.-L., Nakanishi, S., Guillemot, F. and Kageyama, R. (1996a). Mammalian *hairy* and *Enhancer of Split* homolog 1 regulates differentiation of retinal neurons and is essential for eye morphogenesis. *Neuron* **16**, 723-734.

Tomita K., Nakanishi, S., Guillemot, F. and Kageyama, R. (1996b). Mash1 promotes neuronal differentiation in the retina. *Genes Cells* **1**, 765-774.

Treisman, J., Morabito, M. A. and Barnstable, C. (1988). Opsin expression in the rat retina is developmentally regulated by transcription activation. *Mol. Cell. Biol.* **8**, 1570-1579.

Turner, D. L. and Cepko, C. L. (1987). A common progenitor for neurons and glia persists in rat retina late in development. *Nature* **328**, 131-136.

Turner, D. L., Snyder, E. Y. and Cepko, C. L. (1990). Lineage-independent determination of cell type in the embryonic mouse retina. *Neuron* **4**, 833-45.

Turner, D. L. and Weintraub, H. (1994). Expression of achaete-scute homolog 3 in Xenopus embryos converts ectodermal cells to a neural fate. *Genes Dev.* **8**, 1434-1447.

Watanabe, T. and Raff, M. C. (1988). Retinal astrocytes are immigrants from the optic nerve. *Nature* **332**, 834-837.

Weintraub, H. (1993). The MyoD family and myogenesis: redundancy, networks, and thresholds. *Cell* **75**, 1241-1244.

Wetts, R. and Fraser, S. E. (1988). Multipotent precursors can give rise to all major cell types of the frog retina. *Science* **239**, 1142-1145.

Yasunami, M., Suzuki, K., Maruyama, H., Kawakami, H., Nagai, Y., Hagiwara, M. and Ohkubo H. (1996). Molecular cloning and characterization of a cDNA encoding a novel basic helix-loop-helix protein structurally related to Neuro-D/BHF1. *Biochem. Biophys. Res. Commun.* **220**, 754-758.

Young, R. W. (1985). Cell differentiation in the retina of the mouse. *Anat. Rec.* **212**, 199-205.

Zimmerman K., Shih J., Bars J., Collazo A. and Anderson D. J. (1993). XASH-3, a novel Xenopus achaete-scute homolog, provides an early marker of planar neural induction and position along the mediolateral axis of the neural plate. *Development* **119**, 221-232.